nature geoscience

LETTERS

PUBLISHED ONLINE: 16 FEBRUARY 2015 | DOI: 10.1038/NGEO2372

Water contents of Earth-mass planets around M dwarfs

Feng Tian[1]* and Shigeru Ida[2]

Efforts to identify habitable extrasolar planets have focused on systems around M dwarfs, faint stars with less than half the solar mass. Habitable planets around M dwarfs are thought to be more plentiful and easier to detect than those orbiting Sun-like G dwarfs[1–4]. However, unlike G dwarfs, M dwarfs experience a prolonged decline in luminosity early in their history, leading to an inward migration of the habitable zone to where planets may have lost their water through dissociation and hydrodynamic escape. Water-poor planets, such as Venus, are considered uninhabitable. In contrast, planets with too much water (>1 wt%) would lack continents[5], leading to climate instability[6] and nutrient limitation problems[7]. Here we combine a numerical planet population synthesis model with a model for water loss to show that the evolution of stellar luminosity leads to two types of planets of Earth-like mass (0.1 to 10 Earth masses) in the habitable zones around M dwarfs: ocean planets without continents, and desert planets, on which there are orders of magnitude less surface water than on Earth. According to our simulations, Earth-mass planets with Earth-like water contents are rare around M dwarfs and occur 10–100 times less frequently than around G dwarfs. We suggest that stars close to the size of the Sun should be the primary targets for detecting Earth-like planets.

It has been well known for decades that the luminosity evolution of M dwarfs is different from that of G dwarfs during the pre-main-sequence (PMS) phase[8–11]: the luminosity of a G dwarf such as our Sun remains almost constant during the PMS phase except for the first few Myr; in contrast the luminosity of an M dwarf decreases by more than one order of magnitude during its PMS phase. As a result, planets in the habitable zones of main-sequence M dwarfs were much closer to the stars than the inner edge of the habitable zone of PMS M dwarfs (Supplementary Methods). Such planets should have water-rich atmospheres during their stars' PMS phase and could have lost their water through hydrodynamic escape of hydrogen and oxygen atoms produced through rapid photodissociation of water molecules. Although there has been a recent study on the water contents of planets much closer to G dwarfs than the habitable zone is[12], until now no study has investigated how the early luminosity evolution of low-mass stars could have impacted the surface water contents of their habitable-zone planets.

Here we apply a water loss model on planetary bodies produced in a planet population synthesis model[13] with stellar masses = 0.3, 0.5 and 1 $M_{\odot}$ (see Methods for model details). Figure 1a–c shows the water mass fractions (the ratios between water mass and planet mass) of Earth-mass planets from the planet population synthesis model alone (no stellar luminosity evolution or water loss considered) 90 Myr after the stars enter the PMS, when the strong XUV flux starts to decay and the stellar luminosity of M dwarfs is stable. Many Earth-mass planets have migrated inwards from outer regions and are piled up near the disk inner edge at ~0.04 AU. Significant fractions of the planets migrate from the regions even beyond the ice line to have water mass fractions >10% for M dwarfs where the disks are relatively cool and the ice lines are closer to the stars. Because coagulations between rocky and icy planets occur, the water content distribution of Earth-mass planets around the water mass fraction of the Earth (10^{-4}) is continuous, especially in the corresponding habitable zones (0.12–0.23, 0.23–0.43 and 0.96–1.8 AU for 0.3, 0.5 and 1 $M_{\odot}$ stars respectively[14]). This distribution is almost independent of the orbital migration model (see Methods).

Figure 1d–f shows the water mass fractions of Earth-mass planets after stellar luminosity evolution and water loss are considered. The impact of stellar luminosity evolution is clear: first, Earth-mass planets with water mass fraction >10% still retain their water because the available stellar XUV energy is inadequate to remove large quantities of water from them; second, Earth-mass planets at close-in orbits lose water so efficiently that gaps are formed in the previously continuous water content distributions at these orbits for low-mass stars. Most of the planets with a close-to-Earth mass and a water mass fraction <1% in Fig. 1a–c move to the regions below 10^{-12} in Fig. 1d–f. For 0.3 $M_{\odot}$ stars, the gap coincides with the habitable zone is during the main sequence phase—the Earth-mass planets in the habitable zone of 0.3 $M_{\odot}$ stars are either ocean planets without continents or dune planets containing extremely low amounts of water.

The bimodal water content distributions of Earth-mass planets in the habitable zones of low-mass stars are better shown in the top and middle panels of Fig. 2 (green bars). The two vertical dotted lines represent the surface water mass fractions of the Earth ($\sim 2 \times 10^{-4}$) and Venus ($\sim 5 \times 10^{-9}$; the detected water mass fraction in the venusian atmosphere[15]) respectively. Among 69,000 planetary bodies in 1,000 systems of 0.3 $M_{\odot}$ stars, there are 5,000 Earth-mass planets; 55 of them in the habitable zone. Among these Earth-mass planets in the habitable zone, 31 are ocean planets, 23 are dune planets and just 1 has an Earth-like water content (water mass fraction between 0.01 and 5×10^{-9}). For 0.5 $M_{\odot}$ stars, the gap in Fig. 1 is mainly at <0.4 AU and for a water mass fraction $<10^{-4}$. Among 75,000 planetary bodies in the 1,000 systems of 0.5 $M_{\odot}$ stars, there are >9,000 Earth-mass planets; 292 of them are in the habitable zone. Among the Earth-mass planets in the habitable zone, 60 are ocean planets, 220 are dune planets and just 12 have an Earth-like water content.

In contrast, the water content distribution of Earth-mass planets in the habitable zone of 1 $M_{\odot}$ stars is continuous (green bars in Fig. 2c), although water loss also occurs on these planets at <0.5 AU orbits. Among 38,000 planetary bodies in the 1,000 systems of 1 $M_{\odot}$

[1]Ministry of Education Key Laboratory for Earth System Modeling, Center for Earth System Science, Tsinghua University, Beijing 100084, China. [2]Earth-Life Science Institute, Tokyo Institute of Technology, Tokyo 152-8550, Japan. *e-mail: tianfengco@tsinghua.edu.cn

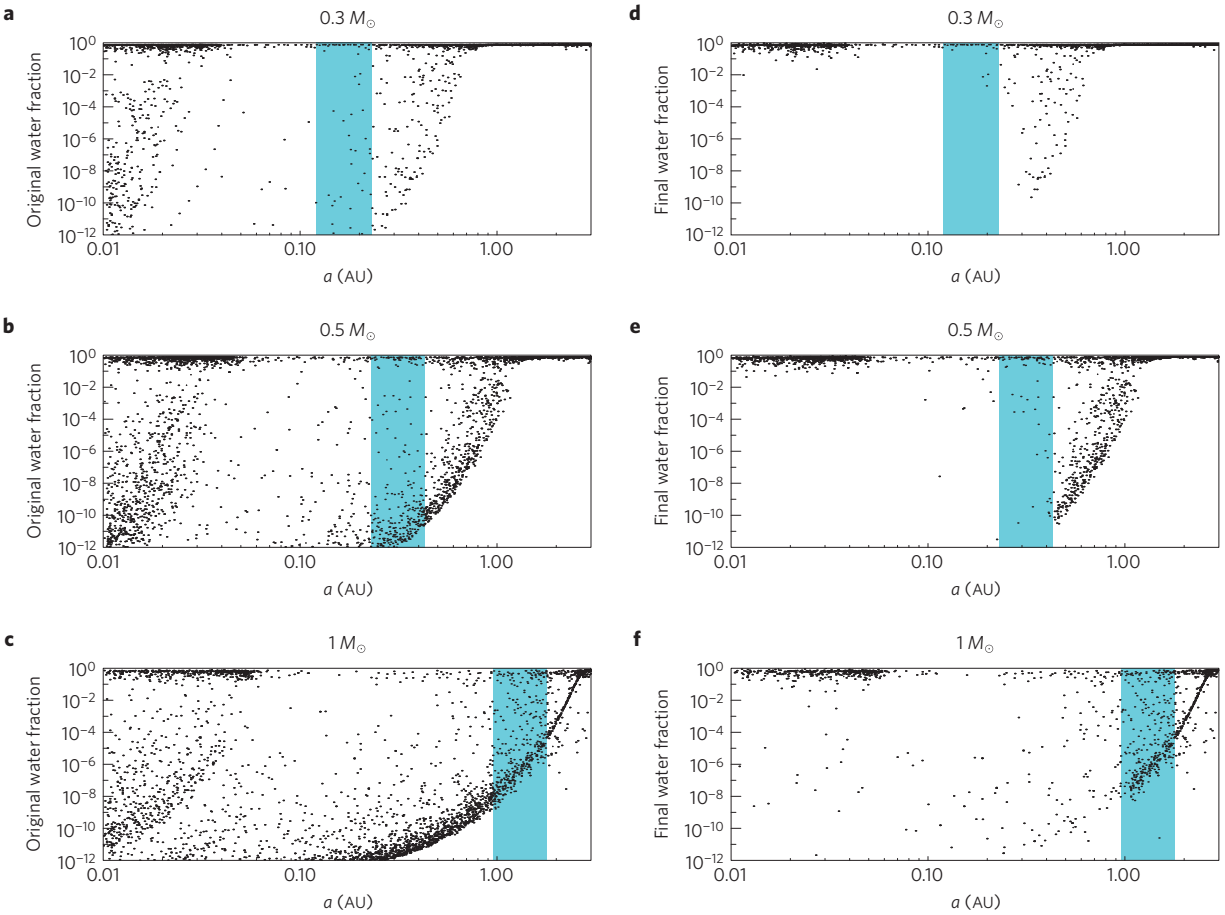

Figure 1 | Water mass fractions versus orbital distances of Earth-mass planets 90 Myr after entering the PMS. a–c, Results without considering the PMS stellar luminosity evolution and water loss. **d–f**, Results considering the stellar luminosity evolution and water loss. The habitable zones of the stars in the main sequence phase are marked by blue shaded areas. Stellar masses are marked in the panels.

stars, there are ~8,000 Earth-mass planets; 407 of them in the habitable zone. Among the latter, 91 are ocean planets, 45 are dune planets and 271 have an Earth-like water content.

The red bars in Fig. 2 are the results in our standard models with the overall escape efficiency $\epsilon = 10\%$ (see Methods) and $L_{xuv}/L_{total} = 10^{-3}$ during the PMS phase (where L_{xuv} and L_{total} are the XUV and total luminosities of the host stars), which is possible for some young active M dwarfs. Using a higher XUV level does not change the water content distributions. Most recent study on hydrodynamic escape from low-mass planets[16] suggests that ϵ is between 5 and 20%. The blue bars in Fig. 2 are the results in models with a lower $L_{xuv}/L_{total} = 10^{-5}$ and $\epsilon = 1\%$ (a most optimistic case for preserving planet water contents). For 0.3 $M_\odot$ stars, the number of Earth twins increases to 4 and the corresponding Earth-twin occurrence rate is 0.4%. For 0.5 $M_\odot$ stars, the number of Earth twins increases to 21—an occurrence rate of 2%. In comparison, there are 274 Earth twins around 1.0 $M_\odot$ stars in this case. The statistics of ocean planets and dune planets in all cases remain similar to those in the standard model. Thus the existence of a bimodal water content distribution on Earth-mass planets in the habitable zones of low-mass stars is robust.

The planet population synthesis model predicts that the occurrence rate of Earth-mass planets in the habitable zones of low-mass stars is ~5% and ~30% for 0.3 and 0.5 $M_\odot$ stars respectively, which is close to the 15^{+13}_{-6}% estimate based on Kepler observations of M dwarfs[4]. However, the occurrence rates of Earth twins in the standard case with $\epsilon = 10\%$ and $L_{xuv}/L_{total} = 10^{-3}$ are only 1% and 0.1% for 0.5 $M_\odot$ and 0.3 $M_\odot$ stars respectively. In contrast, PMS stellar luminosity evolution does not impact planet habitability of 1 $M_\odot$ stars and the occurrence rate of Earth twins for 1 $M_\odot$ stars could exceed 20%, 10–100 times greater than that for M dwarfs.

Our model further shows that the gaps in water content distributions of planetary bodies with masses less than 0.1 Earth mass are even wider and more substantial than those of Earth-mass planets. Thus the probability for Earth-mass planets to obtain water through giant impacts with smaller planetary embryos would be low. However, the possibility for dry Earth-mass planets around M dwarfs to obtain Earth-like water content through collisions with comets, especially in the existence of nearby-passing stars and/or giant planets, cannot be ruled out by our model.

One underlying assumption of the model is that all water on the planets is at the surface during the PMS phase. Earth-mass planets may retain some water in the mantle during the PMS phase and release water to the surface at a later time. Recent studies[17,18] show that the length of the magma-ocean phase is determined by both planetary initial water content and the radiation the planet receives from its star. Comparisons between the time evolution of magma oceans[18] and the stellar luminosity evolution (Supplementary Methods) suggest that the magma-ocean phase is of the order of 1 Myr for habitable-zone planets around G dwarfs but several tens of Myr for habitable-zone planets around M dwarfs. The long magma-ocean phase of planets under strong stellar irradiance limits the amount of water in the solid mantle after the magma-ocean phase to <0.1 Earth ocean[17] and such a planet may have water locked in its mantle but little surface water. The dune planets

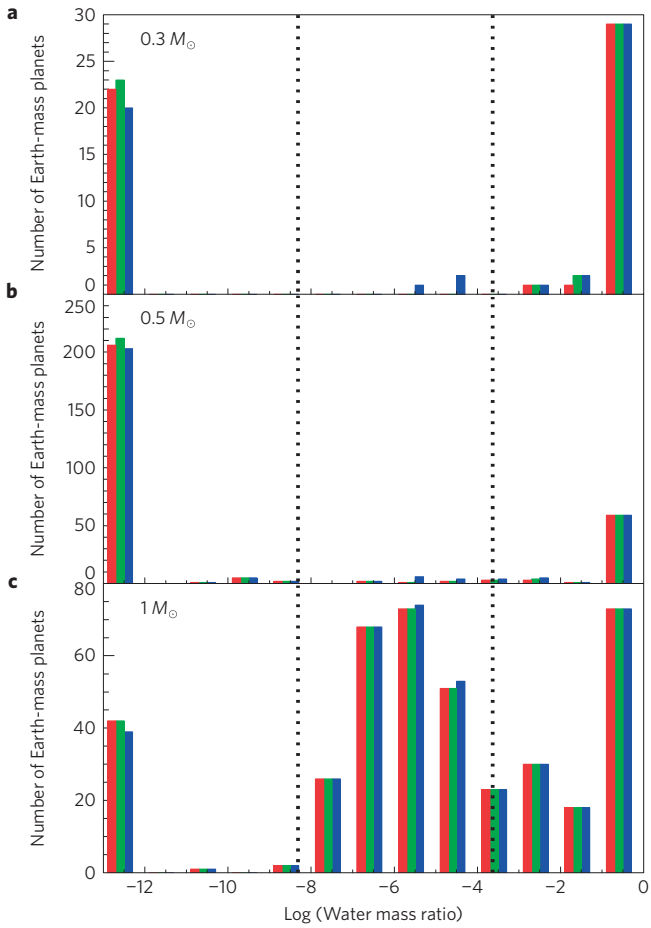

Figure 2 | Water fraction distributions of habitable-zone Earth-mass planets 90 Myr after the stars enter the PMS. a–c, 0.3, 0.5 and 1 $M_\odot$ stars, respectively. Green bars $L_{xuv}/L_{total}=10^{-4}$ and $\epsilon=10\%$; red bars $L_{xuv}/L_{total}=10^{-3}$ and $\epsilon=10\%$; blue bars $L_{xuv}/L_{total}=10^{-5}$ and $\epsilon=1\%$. Planets with water mass content $<10^{-12}$ are accumulated to the leftmost bars. The two vertical dotted lines represent the surface water mass fractions of the Earth and the detected water mass fraction in the venusian atmosphere.

around M dwarfs could become Venus twins with water-poor and CO_2-dominant atmospheres as the result of an inhibited hydrologic cycle. The issues of how efficiently and when the water retained in the mantle would be released to the planet surface need to be studied in future work, for which the bimodal water content distribution of Earth-mass planets at the end of PMS phase of M dwarfs provides necessary initial and boundary conditions.

Earth twins, dune planets and ocean planets could be distinguished from one another by bulk density measurements and multi-band spectral observations. Within the next decade, TESS, Plato, and other missions/facilities will play important roles in the search for Earth twins around nearby stars. Roughly 60% of all stars within 30 light years of the Sun are $\leq$0.3 $M_\odot$, 35% are between 0.3 and 1 $M_\odot$, and 20% are between 0.6 and 1 $M_\odot$. If our estimate on water contents of Earth-mass planets is correct, the last group of stars should be the primary targets for true Earth-twin searches in the coming decades.

Note added in proof: While this Letter was in press, we noticed a paper that has similar motivation but did not use a planet population synthesis model to obtain the bimodal water content distribution: Ramirez, R. M. & Kaltenegger, L. The habitable zones of pre-main-sequence stars. *Astrophys. J. Lett.* **797,** L25 (2014).

Methods

Water loss from water-vapour-rich atmospheres would be controlled by the energy available to lift hydrogen and oxygen atoms from the gravity fields, with stellar XUV photons being the most important energy source. Although the details of hydrodynamic escape from planetary atmospheres are not well established, the observed mass-size distribution of low-mass Kepler planets[19] demonstrates that the following energy-limited escape formula

$$F=\frac{L_{xuv}\epsilon}{16\pi ED^2}$$

with $\epsilon=10\%$ being appropriate to describe the overall evolution of the observed mass-size distribution of low-mass Kepler planets. Here F is the escape flux of hydrogen in $cm^{-2}\,s^{-1}$, L_{xuv} is the XUV luminosity of the star in $ergs\,s^{-1}$, D is orbital distance of the planets, E is the gravitation energy of H atoms, and ϵ is the overall escape efficiency, which describes how much XUV photon energy ends up in the energy consumed by the hydrodynamic escape.

Note that ϵ is neither the photoelectron heating efficiency nor the heating efficiency. The XUV heating efficiency is 15$\sim$25% for CO_2-dominant atmospheres[20], 30$\sim$40% for N_2–O_2-dominant atmospheres[21], and 45–65% for hydrogen-dominant atmospheres[22]. In the extreme case oxygen could be carried out by the escaping hydrogen and the ratio between hydrogen and oxygen atoms could reach 2:1. With abundant oxygen in the upper atmosphere, the escape efficiency could be different from that in a hydrogen-dominated upper atmosphere, but should be within one order of magnitude despite the large composition difference. Thus $\epsilon=1\%$ and 10% are used in this work to explore how different escape efficiency influences the conclusion of this work.

The ratios L_{XUV}/L_{total} of M dwarfs are 10 to 1,000 times greater than that of the Sun ($\sim10^{-6}$) today[23]. Considering the fact that the young Sun was $\sim$100 brighter in XUV during its first 100 Myr (ref. 24), $L_{xuv}/L_{total}=10^{-4}$ is used for PMS M dwarfs in the standard case of this work. Model runs with different XUV levels and different escape efficiencies are carried out and the results are included in Fig. 2.

In the planet population synthesis model, 1,000 systems with different initial disk surface densities are modelled for each stellar mass. The initial surface density is distributed between 0.1 and 40 times the minimum-mass solar nebula model[25] for solar-mass stars, and power laws with indices of -1.5 and -1 are used for the initial surface density distributions of the solid material and the gas respectively. The mean surface density is proportional to the square of the stellar mass. A Gaussian distribution with mean -0.1 and standard deviation 0.2 is used for the metallicity [= $\log_{10}$(solid to gas ratio scaled by the Solar value)]. We track the growth of the planets through accretion of planetesimals, other planets and disk gas[13], and the evolution of their water content between 5 Myr and 90 Myr after the stars enter the PMS phase. Inward orbital migration of the planets due to gravitational interaction with disk gas is given by the formula for isothermal disks[26] with a deceleration factor of 10. The detailed distribution of the Earth-mass planets may depend on the orbital migration model and gravitational perturbations from gas giants (the formation probability of gas giants is sensitively affected by the migration model for their cores). However, as long as we are concerned with the distribution of water content in close-in Earth-mass planets, the results are not significantly changed by a different choice of the migration model[27,28]. Although the up-to-date migration formula for non-isothermal disks[28] shows outward migration, the outward migration is limited in some ranges of disk and planetary parameters[29]. Many Earth-mass planets eventually migrate inwards as a result of disk evolution and the migration would be stalled near the inner disk edge.

Received 1 September 2014; accepted 20 January 2015; published online 16 February 2015; corrected online 19 February 2015

References

1. Howard, A. W. Observed properties of extrasolar planets. *Science* **340,** 572–576 (2013).
2. Johnson, J. Warm planets orbiting cool stars. *Phys. Today* **67,** 31–36 (March, 2014).
3. Howard, A. W. *et al.* Planet occurrence within 0.25 AU of solar-type stars from Kepler. *Astrophys. J. Suppl.* **201,** 15 (2012).
4. Dressing, C. D. & Charbonneau, D. The occurrence rate of small planets around small stars. *Astrophys. J.* **767,** 95 (2013).
5. Cowan, N. B. & Abbot, D. S. Water cycling between ocean and mantle: Super-Earths need not be waterworlds. *Astrophys. J.* **781,** 27 (2014).
6. Abbot, D. S., Cowan, N. B. & Ciesla, F. J. Indication of insensitivity of planetary weathering behavior and habitable zone to surface land fraction. *Astrophys. J.* **756,** 178 (2012).
7. Dohm, J. & Maruyama, S. Habitable trinity. *Geosci. Front.* **6,** 95–101 (2015).

8. Hayashi, C. Stellar evolution in early phases of gravitational contraction. *Publ. Astron. Soc. Jpn* **13,** 450–452 (1961).
9. Di Criscienzo, M., Ventura, P. & D'Antona, F. Updated pre-main sequence tracks at low metallicities for $0.1 \leq M/M_{\odot} \leq 1.5$. *Astron. Astrophys.* **496,** 223–227 (2009).
10. Paxton, B. *et al.* Modules for experiments in stellar astrophysics (MESA). *Astrophys. J. Suppl.* **192,** 3 (2011).
11. Tognelli, E., PradaMoroni, P. G. & Degl'Innocenti, S. The Pisa pre-main sequence tracks and isochrones A database covering a wide range of Z, Y, mass, and age values. *Astron. Astrophys.* **533,** A109 (2011).
12. Kurosaki, K., Ikoma, M. & Hori, Y. Impact of photo-evaporative mass loss on masses and radii of water-rich sub/super-Earths. *Astron. Astrophys.* **562,** A80 (2014).
13. Ida, S., Lin, D. N. C. & Nagasawa, M. Toward a deterministic model of planetary formation. VII. Eccentricity distribution of gas giants. *Astrophys. J.* **775,** 42 (2013).
14. Kopparapu, R. K. *et al.* Habitable zones around main-sequence stars: Dependence on planetary mass. *Astrophys. J. Lett.* **787,** L29 (2014).
15. Mills, F. P., Esposito, L. W. & Yung, Y. L. in *Exploring Venus as a Terrestrial Planet* Vol. 176 (eds Esposito, L. W., Stofan, E. R. & Cranvens, T. E.) 73–100 (Geophysical Monograph Series, AGU, 2007).
16. Owen, J. E. & Jackson, A. P. Planetary evaporation by UV and X-ray radiation: Basic hydrodynamics. *Mon. Not. R. Astron. Soc.* **425,** 2931–2947 (2012).
17. Hamano, K., Abe, Y. & Genda, H. Emergence of two types of terrestrial planet on solidification of magma ocean. *Nature* **497,** 607–611 (2013).
18. Lebrun, T. *et al.* Thermal evolution of an early magma ocean in interaction with the atmosphere. *J. Geophys. Res.* **118,** 1–22 (2013).
19. Lopez, E. D. & Fortney, J. J. The role of core mass in controlling evaporation: The Kepler radius distribution and the Kepler-35 density dichotomy. *Astrophys. J.* **776,** 2 (2013).
20. Fox, J. L. Heating efficiencies in the thermosphere of Venus reconsidered. *Planet. Space Sci.* **36,** 37–46 (1988).
21. Roble, R. G. in *The Upper Mesosphere and Lower Thermosphere: A Review of Experiment and Theory* Vol. 87 (eds Johnson, R. M. & Killeen, T. L.) 1–21 (Geophys. Monogr. Ser., AGU, 1995).
22. Koskinen, T. T., Yelle, R. V., Harris, M. J. & Lavvas, P. The escape of heavy atoms from the ionosphere of HD209458b. II. Interpretation of the observations. *Icarus* **226,** 1695–1708 (2013).
23. Scalo, J. *et al.* M stars as targets for terrestrial exoplanet searches and biosignature detection. *Astrobiology* **7,** 85–171 (2007).
24. Ribas, I., Guinan, E. F., Güdel, M. & Audard, M. Evolution of the solar activity over time and effects on planetary atmospheres I. High energy irradiances (1–1700 A). *Astrophys. J.* **622,** 680–694 (2005).
25. Hayashi, C. Structure of the solar Nebula, growth and decay of magnetic fields and effects of magnetic and turbulent viscosities on the Nebula. *Prog. Theor. Phys. Suppl.* **70,** 35–53 (1981).
26. Tanaka, H., Takeuchi, T. & Ward, W. R. Three-dimensional interaction between a planet and an isothermal gaseous disk. I. Corotation and Lindblad torques and planet migration. *Astrophys. J.* **565,** 1257–1274 (2002).
27. Ida, S. & Lin, D. N. C. Toward a deterministic model of planetary formation. VI. Dynamical interaction and coagulation of multiple rocky embryos and super-Earth systems around solar-type stars. *Astrophys. J.* **719,** 810–830 (2010).
28. Paardekooper, S-J., Baruteau, C. & Kley, W. A torque formula for non-isothermal Type I planetary migration—II. Effects of diffusion. *Mon. Not. R. Astron. Soc.* **410,** 293–304 (2011).
29. Kretke, K. A. & Lin, D. N. C. The importance of disk structure in stalling type I migration. *Astrophys. J.* **775,** 74 (2012).

Acknowledgements

We thank J. L. Lissauer and I. Pascucci for stimulating discussions. We thank D. S. Abbot for a constructive review. F.T. is supported by the National Natural Science Foundation of China (41175039) and the Startup Fund of the Ministry of Education of China. S.I. is supported by MEXT/JSPS KAKENHI Grant no. 23103005.

Author contributions

Both authors designed the project. S.I. carried out the planet population synthesis modelling and F.T. carried out the water loss modelling and analysed the data. Both authors wrote the manuscript.

Additional information

Supplementary information is available in the online version of the paper. Reprints and permissions information is available online at www.nature.com/reprints. Correspondence and requests for materials should be addressed to F.T.

Competing financial interests

The authors declare no competing financial interests.

ERRATUM

Water contents of Earth-mass planets around M dwarfs

Feng Tian and Shigeru Ida

Nature Geoscience https://dx.doi.org/10.1038/ngeo2372 (2015); published online 16 February 2015; corrected online 19 February 2015.

In the version of this Letter originally published, in Fig. 1, the *x* axes should have been labelled '*a* (AU)' and the *y* axes should have indicated water mass fraction. These errors have been corrected in all versions of the Letter.